Geological Survey of Finland

Bulletin 277

A contribution to the mineralogy of iron-magnesium silicates, especially pyroxenes, contained in certain noritic rocks in Central Finland

by Atso Vorma

Geologinen tutkimuslaitos · Espoo 1975

Geological Survey of Finland, Bulletin 277

A CONTRIBUTION TO THE MINERALOGY OF IRON-MAGNESIUM SILICATES, ESPECIALLY PYROXENES, CONTAINED IN CERTAIN NORITIC ROCKS IN CENTRAL FINLAND

BY

ATSO VORMA

WITH 16 FIGURES AND 8 TABLES IN THE TEXT

GEOLOGINEN TUTKIMUSLAITOS
ESPOO 15 (OTANIEMI)
1975

Vorma, A. 1975: A contribution to the mineralogy of iron-magnesium silicates, especially pyroxenes, contained in certain noritic rocks in Central Finland. *Geological Survey of Finland, Bulletin 277.* 25 pages, 16 figures, 8 tables.

Orthopyroxene, clinopyroxene and clinoamphibole from noritic rocks belonging to the Main Sulphide Ore Belt in Finland were studied by the X-ray single-crystal, electron microprobe and optical methods. It was detected that the orthopyroxene, the composition of which ranges from bronzite to ferrohypersthene, is in fact an oriented intergrowth of up to four mineral phases, viz., of orthopyroxene, clinopyroxene, clinoamphibole and ilmenite. The clinopyroxene (augite) was shown to be an oriented intergrowth of clinopyroxene and clinoamphibole, in some instances also of orthopyroxene (and leucoxene). The clinoamphibole (normal hornblende) is shown to have many modes of occurrence, either intergrown with clinopyroxene or forming grains without any intergrowths whatsoever.

Also some biotite data are given, *e.g.*, on the basis of a microprobe analysis.

The study shows that the Fe-Mg silicate assemblages in the noritic rocks investigated are in disequilibrium. Submagmatic (deuteric) reactions or metamorphic reactions connected with the Svecokarelidic orogeny have led to the present mineral assemblages and adjusted the composition of the Fe-Mg silicates.

ISBN 951-690-018-6

Helsinki 1975. Valtion painatuskeskus

CONTENTS

INTRODUCTION

In connection with the mapping program of the Geological Survey in the early 1960s, a series of gabbroic rock samples in the Pieksämäki map sheet area (see, Vorma 1971) were collected. Some of these samples are described in this study. The Pieksämäki area lies at the southwest margin of the Main Sulphide Ore Belt, as defined by Kahma (1973).

The Main Sulphide Ore Belt runs from Lake Ladoga diagonally in a SE-NW direction across Finland. Hypersthene-bearing plutonic rocks are among the characteristic features of this belt. Their distribution and concentration within the belt was first discussed by Wahl in 1963. Recently, Häkli (1970, 1971) and Gaál (1972) have studied the correlation between the Ni-Cu mineralizations and the basic-to-ultrabasic, mostly hypersthene-bearing intrusive rocks along the belt. The basic plutonic rocks in the southeastern part of the belt have been recently described as synorogenic Svecokarelidic intrusions (Gaál and Rauhamäki 1971). Rauhamäki (*op.cit.*, p. 287) regards them as mangeritic intrusive rocks. In this mangeritic series, Rauhamäki distinguishes the following rock types: ultrabasic intrusive rocks (peridotite, hypersthenite and hornblendite), gabbros (olivine gabbro, norite, pyroxene gabbro and uralite gabbro—hornblende gabbro), diorites (pyroxene diorite, biotite-hornblende diorite and hornblende-cummingtonite diorite), quartz diorites (pyroxene quartz diorite and hornblende quartz diorite) and charnockites. Furthermore, all these groups form a comagmatic differentiation series.

Some mineralogical data on the Fe-Mg silicates occurring in these hypersthene-bearing rock series have been published earlier by, *e.g.*, Savolahti (1966), Häkli (1968) and Saltikoff (1971).

Savolahti (1966) described the mineralogy of the Salmenkylä gabbro and its pegmatoid differentiates in the Kangasniemi area. In his study, the chemical composition of diopsidic augite and hypersthene was reported and the oriented intergrowth of these minerals discussed. Saltikoff (1971) used the electron microprobe method to study the chemical composition of certain iron-magnesium minerals from the Virtasalmi area (see, Hyvärinen 1969).

The original purpose of the present study was to find out the extent to which the Fe-Mg silicate assemblages represent mineral parageneses in equilibrium and the kind of conclusions about the petrogenesis of these very important gabbroic

rocks that can be drawn from the study of their Fe-Mg silicates. Therefore this study amounts to a combination of microscopic, X-ray single-crystal and microprobe work on hypersthene, augite, hornblende and biotite contained in selected hypersthene-bearing gabbroic rocks from the area of the Pieksämäki map sheet (Vorma 1971). During the work, it turned out that the petrogenetic interpretation requires further investigation. The rocks studied, however, are of such great economic interest that it is felt justified to publish the mineralogical data without far-reaching conclusions.

DESCRIPTION OF THE SAMPLES

The sampling sites are marked on the geological sketch map in Fig. 1, the specimens collected are listed in Table 1. The rock samples were taken from five different norite bodies, varying in diameter from a few hundred meters to more than one kilometer and having a circular or oval shape. Gravimetric investigations of similar norites to the south of the study area indicate their thickness to vary between only some tens of meters and several hundred meters (Saltikoff 1971).

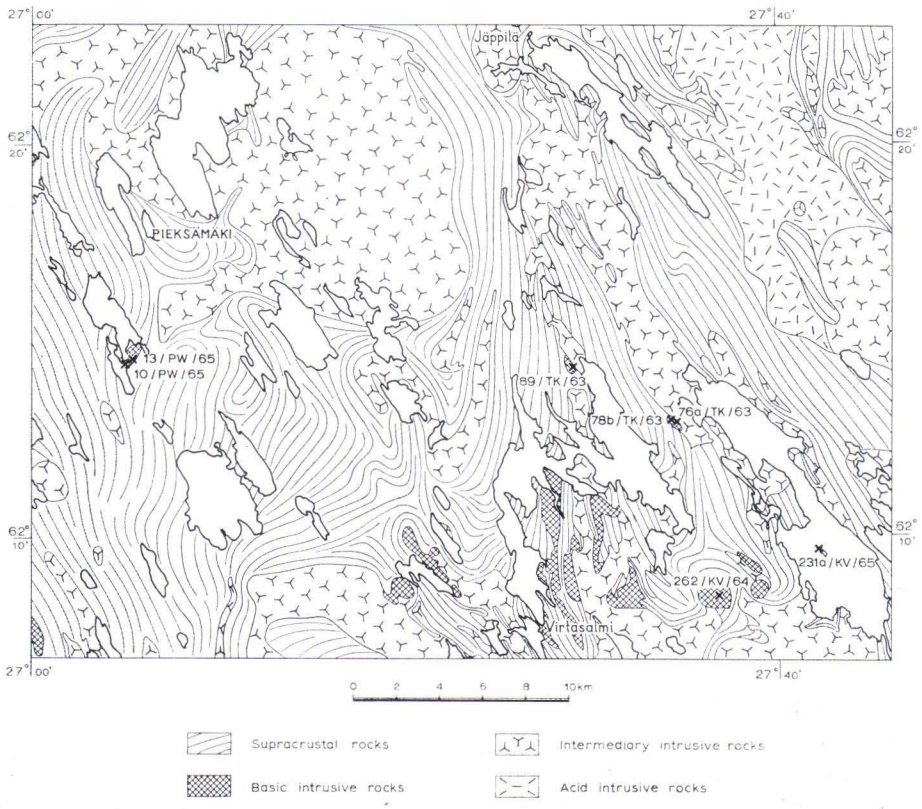

FIG. 1. Geological sketch map simplified from the Geological Map of Finland, sheet 3232, Pieksämäki (Vorma 1971). The sampling sites are indicated in the map.

TABLE 1.

List of norite specimens studied for pyroxenes and amphiboles from Pieksämäki map sheet area, Central Finland.

76a/TK/63	Gabbronorite: medium-grained, ophitic in texture; olivine-bearing; plagioclase An_{48-74}; reddish-brown biotite.
78b/TK/63	Gabbronorite: medium-grained; rich in epidote; plagioclase An_{76-83}.
89a/TK/63	Gabbronorite: small-grained; olivine-bearing; plagioclase An_{65-67}; biotite is present.
262/KV/64	Leuconorite: medium to coarse-grained, ophitic; plagioclase An_{65-70}.
231a/KV/67	Gabbronorite: medium-grained; plagioclase An_{54-72}; almost uniaxial biotite present.
10/PW/65	Pyroxene-hornblende gabbronorite: medium-grained; plagioclase An_{40-61}; biotite is present.
13/PW/65	Pyroxene-hornblende gabbronorite: medium-grained; plagioclase An_{40-65}.

The rock, illustrated in Fig. 2, in which the orthocumulate texture is well developed, was subjected to a wet chemical analysis. The results are given in Table 2. The analytical results and the CIPW norm calculated from them show that the rock was enriched in calcic plagioclase as compared with the average composition of gabbroic rocks. Analogous counterparts are, *e.g.*, the cumulate rocks of Skaergaard (Wager and Brown 1967).

TABLE 2.

Chemical composition, CIPW norm and Niggli numbers of the leuconorite, sample No. 262/KV/64, from Harjärvi, Joroinen. Anal. Pentti Ojanperä.

		CIPW norm		Niggli numbers	
SiO_2	52.27	Q	.07	si	132.1
TiO_2	.24	or	2.36	al	36.1
Al_2O_3	24.23	ab	27.42	fm	27.1
Fe_2O_3	.67	an	50.39	c	28.2
FeO	3.33	di	1.00	alk	8.6
MnO	.07	hy	17.14	qz	—2.22
MgO	4.95	mt	.97	mg	.69
CaO	10.42	il	.46	k	.075
Na_2O	3.24	ap	.02		
K_2O	.40		99.83		
P_2O_5	.01				
CO_2	.00				
H_2O+	.40	Components of pyroxenes separately			
H_2O-	.08	wo	.52		
	100.31	en	12.33		
		fs	5.29		
		Plag. An_{65}			

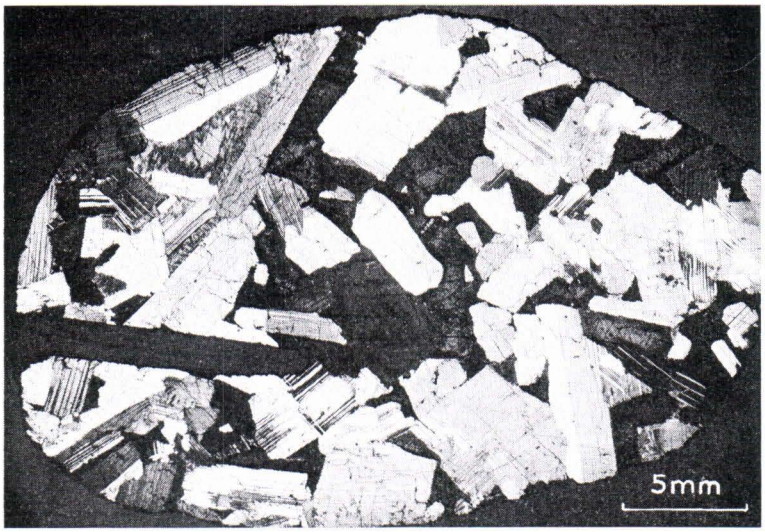

FIG. 2. Leuconorite showing a well-developed orthocumulate texture. The intercumulus material is composed mainly of orthopyroxene with some clinopyroxene. Sample No. 262/KV/64. Crossed nicols.

FIG. 3. Gabbronorite showing a plagioclase mesocumulate texture. The symbols opx, a, hbl, and bi indicate the chemically analyzed orthopyroxene, augite, hornblende and biotite grains, respectively. Sample No. 76a/TK/63. Crossed nicols.

Characteristic textures in the present samples are those of a plagioclase orthocumulate (Fig. 2). In certain samples, olivine also occurs as a cumulus crystal. When the intercumulus material is scanty, the rock gives the impression of a plagioclase mesocumulate (Fig. 3). In both orthocumulate and mesocumulate, orthopyroxene and clinopyroxene occur as large poikilitic crystals, which give the rock a subophitic texture.

The names applied in this paper to the rocks follow the recommendations of the IUGS Subcommission on the Systematics of Igneous Rocks (see, Streckeisen 1973). The norite samples are therefore designated as leuconorite, gabbronorite and pyroxene-hornblende gabbronorite.

DESCRIPTION OF MINERALS

Orthopyroxene

The orthopyroxene (Figs. 4—7) occurs as large poikilitic grains enclosing plagioclase for the most part, but also olivine. In some cases, there is an oriented overgrowth of biotite against plagioclase (Figs. 4—5).

Under the microscope, the mineral appears to be weakly pleochroic. Table 3 gives the range of optical axial angles measured by the Universal Stage and the composition of the mineral as deduced from the diagrams published by Deer *et al.* (1963, p. 28). The scatter in the $2V\alpha$ is quite large. This is not, however, necessarily real because of possible interference by the optical properties of the exsolved phases contained in the orthopyroxene.

Under the microscope, the mineral is seen to have a lamellar structure (Figs. 4—7). The lamellae are oriented parallel to the (100) plane of the orthopyroxene and the individual lamellae have a thickness of 1 to 2 μm. A similar lamellar structure has been described elsewhere (see, *e.g.*, Deer *et al.*, 1963, pp. 32—33).

TABLE 3.

The range in $2V\alpha$ of orthopyroxene and the deduced composition.[1])

	1	2	3	4	5	6	7
Range of $2V\alpha$(°)	60—75	72—74	56—74	66—70	56—70	52—57	60—64
Range of composition in mol. % of Fs.	32—21	22—21	36—21	27—24	36—24		
Mean of $2V\alpha$(°) (number of determination)	70 (4)	73 (2)	63 (5)	68 (2)	65 (6)	55 (5)	62 (2)
Composition from $2V\alpha$ (mean)	23	22	29	25	28		

[1]) The composition is given only for those samples for which the ferrosilite content can be safely assumed to be either considerably less than about 50 mol. % or considerably more than 50 mol. %. If there are ambiguities in this respect, concerning the composition of samples Nos. 10 and 13, no unambiguous composition estimate can be given.

1. 76a/TK/63
2. 78b/TK/63
3. 89a/TK/63
4. 262/KV/64
5. 231a/KV/67
6. 10/PW/65
7. 13/PW/65

For characterization of rock samples, see Table 1.

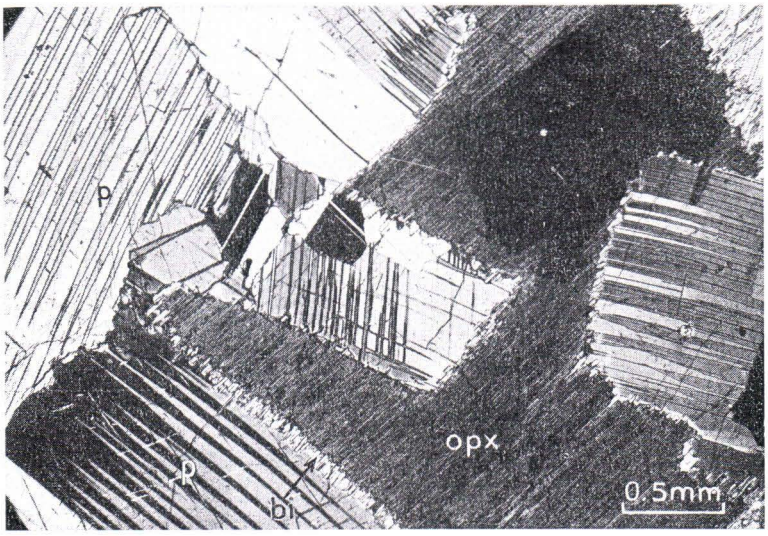

FIG. 4. Lamellar orthopyroxene (opx) with overgrowth of biotite (bi) against plagioclase (p). Sample No. 262/KV/64. Crossed nicols.

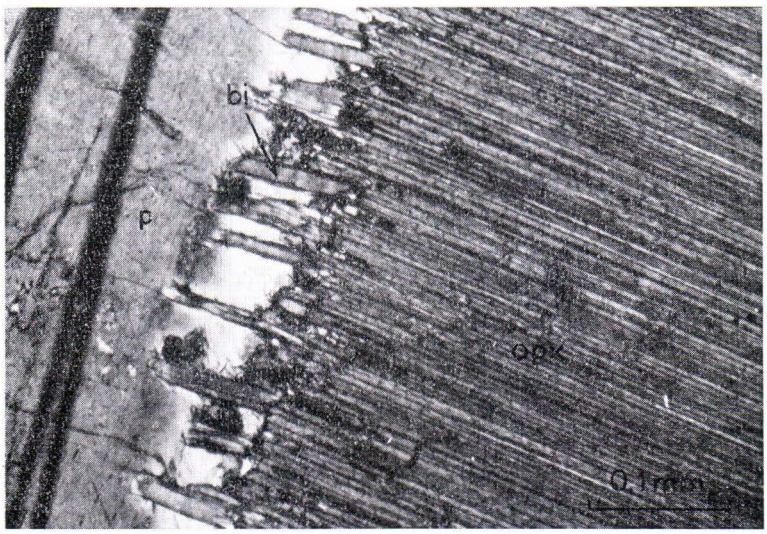

FIG. 5. A detail of Fig. 4 showing the lamellar structure well-developed. opx, orthopyroxene; bi, biotite; p, plagioclase. Crossed nicols.

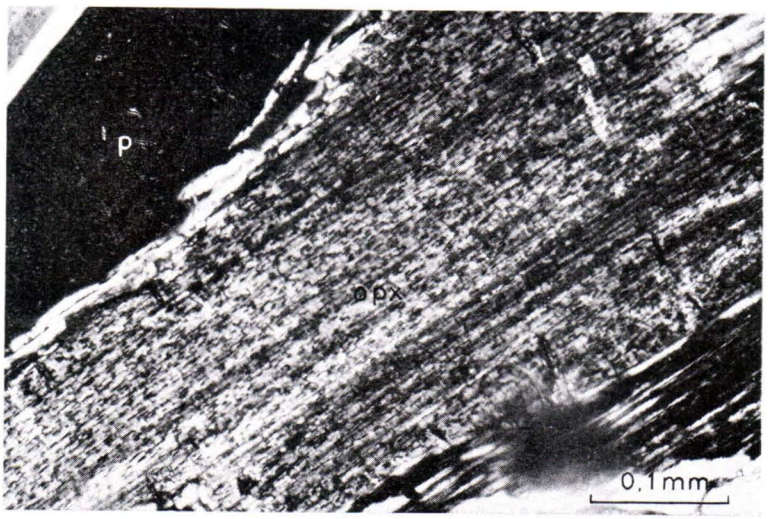

FIG. 6. Lamellar hypersthene (opx) with ilmenite(?) inclusions. p, plagioclase. Sample No. 262/KV/64. Crossed nicols.

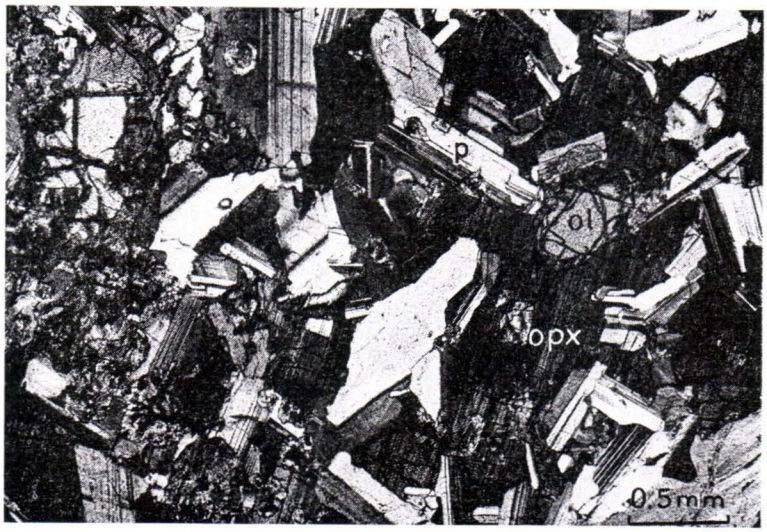

FIG. 7. Lamellar poikilitic hypersthene (opx) with inclusions of olivine (ol), and plagioclase (p). Gabbronorite, sample No. 89a/TK/63. Crossed nicols.

The lamellar intergrowth was studied by X-ray single-crystal methods by taking *a*-axis zero-level and *b*-axis zero-level precession photographs from eight crystal splinters of orthopyroxene. The photographs show that the oriented intergrowhts consist of up to four mineral phases, namely, those of orthorhombic pyroxene, monoclinic pyroxene, hornblende and ilmenite. The results of the measurements of the photographs are given in Table 4.

The film shrinkage was eliminated by recording the orthopyroxene reflections and the silicon standard reflections on the same film. The accuracy in cell dimensions

TABLE 4.

Cell dimensions of host hypersthene and those of augite, hornblende and ilmenite intergrown with hypersthene. Only the cell dimensions are given that are measurable from the *a*-axis and *b*-axis zero level precession photographs from hypersthene. Also the ferrosilite (Fs) content deduced from the cell dimensions in mol. % in the orthopyroxene is given.

		1	2	3	4	5	6	7	8
Hypersthene	a_o	18.30	18.30	18.26	18.29	18.29	18.29	18.34	18.31
	b_o	8.869	8.859	8.871	8.877	8.855	8.875	8.948	8.917
	c_o	5.221	5.212	5.213	5.205	5.206	5.221	5.226	5.221
	Fs (%)	35	31	25	27	25	34	53	43
Augite	a_o	9.750	—	9.757	9.786	9.768	9.735	—	—
	b_o	—	—	—	—	—	—	—	—
	c_o	5.239	—	5.233	(5.296)	5.259	(5.278)	—	—
	β	105°22′	—	105°42′	(105°13′)	(105°23′)	(105°18′)	—	—
	$a_o sin\beta$	9.405	9.397	9.407	9.386	9.376	9.405	—	—
	Remarks	*m*	*vw*	*m*	*w, d*	*m*	*m*	—	—
Hornblende	a_o	—	9.820	—	—	—	—	9.855	9.842
	b_o	—	18.07	—	18.06	18.06	18.09	18.12	18.15
	c_o	—	5.294	—	—	—	—	5.301	5.294
	β	—	105°22′	—	—	—	—	104°42′	105°07′
	$a_o sin\beta$	—	9.557	—	—	9.534	9.527	—	9.543
	Remarks	—	*m*	—	*vw*	*vw*	*w*	*m*	*m*
Ilmenite	a_o	5.095	5.096	5.107	5.084	5.089	5.108	5.093	5.082
	c_o	14.07	14.10	14.03	14.10	14.09	14.09	14.11	14.10
	Remarks	*s*	*s*	*s*	*m*	*m*	*s*	*vw*	*vw*

Remarks: — = the phase in question absent
d = diffuse
vw = very weak
w = weak
m = medium strong
s = strong
} the intensity of reflections of the phase in question

( ) indicates lattice dimensions whose accuracy is poorer than that of others.

1. 76a/TK/63
2. 78b/TK/63
3. 89a/TK/63
4. 262/KV/64-1
5. 262/KV/64-2
6. 231a/KV/67
7. 10/PW/65
8. 13/PW/65

For characterization of rock samples, see Table 1.

of the orthopyroxene is believed to correspond to probable errors of ± 0.020, ± 0.010 and ± 0.005 Å in a_o, b_o and c_o, respectively. In augite, hornblende and ilmenite, the probable errors are larger, because of the diffuse nature of many of the reflections.

The cell dimensions show that the orthopyroxene hosts contain from 25 mol. % to 53 mol. % of the ferrosilite component — from iron-rich bronzite to ferrohypersthene — (Table 4).

The precession photographs show that $c_{opx}//c_{cpx}//c_{amph}//c_{ilmenite}$, in which *opx* = orthopyroxene and *cpx* = clinopyroxene.

The orthopyroxenes of samples Nos. 10 and 13/PW/65, listed in Table 4, turned out to be different from the other orthopyroxenes. The samples [1]) are from one and the same norite body in the western part of the sketch map area (Fig. 1). These orthopyroxenes are characterized by, for example, the following features:

— no clinopyroxene is detected as an oriented intergrowth in them;

— the ilmenite reflections are very weak;

— the hornblende reflections are moderately strong;

— the orthopyroxene is richer in the ferrosilite component that in other samples.

A reason for the differences in the characteristics of the orthopyroxenes in samples 10 and 13, on the one hand, and in the other samples, on the other, could be the different geological environments of the rocks. By and large, the grade of metamorphism and migmatization is higher in the western part of the sketch map area (upper part of the low-pressure amphibolite facies) than in the eastern part. In the east, the noritic rocks resisted metamorphic recrystallization better and they bear the mineral assemblages of a magmatic facies, while in the west the metamorphic mineral facies is more marked.

Some of the orthopyroxenes were subjected to an electron microprobe study. The samples studied and the results obtained are listed in Table 5. A bulk composition was obtained in each case because the resolving power was not high enough to have the host hypersthene solely analyzed. It can be deduced that the compositions vary from bronzite (No. 262/KV/64-3) to ferrohypersthene (231a/KV/64). The high TiO_2 contents are due to ilmenite, the high CaO contents to augite and hornblende, and the Al_2O_3 contents to hornblende. A scanning across the lamellae (sample 89a/TK/63) shows slight fiuctuations in composition: the Al_2O_3 and CaO contents show a positive correlation.

If the intergrowth was produced by exsolution, the high Ca, Al and Ti figures suggest a pigeonite origin for the orthopyroxene. The original pigeonite would have become transformed into orthopyroxene. Augite and ilmenite lamellae exsolved under low fugacity of oxygen conditions. A later increase in the fugacity of H_2O would have catalyzed the uralitization of some exsolved augite. The Ca-poor pyroxenes (Nos. 10 and 13/PW/65, in Table 4), which are richer in the ferrosilite component, seem to represent a lower original crystallization temperature. The fugacity

[1]) Samples 10 and 13 are poor in clinopyroxene. Hornblende, on the other hand, is abundantly present. The clinopyroxene is intensely uralitized.

TABLE 5.

Partial electron microprobe analyses of orthopyroxenes of norites from the Pieksämäki map sheet area.

	1	2	3	4	5	6	7
SiO_2	50.6	49.7	50.2	49.0	48.6	48.5	50.2
TiO_2	.8	.9	1.7—2.5	.8	1.1	.7	.7
Al_2O_3	4.3	4.1	1.3	3.3	3.6	3.7	2.3
FeO	16.0	21.3	22.6	18.8	19.6	16.4	28.3
MnO	.2	.3	.4	.2	.3	.3	.5
MgO	26.8	23.2	24.5	21.8	20.3	27.7	17.6
CaO	2.3±	1.7—2.7	2.8—3.6	4.8	2.5	1.3	1.2
100Fe/Fe+Mg+Mn	25.0	33.8	33.9	32.5	35.0	24.8	47.0
Fe	24.0	32.5	32.1	29.5	33.2	24.3	46.3
Mg	71.6	63.2	62.1	60.9	61.3	73.2	51.2
Ca	4.4	4.3	5.8	9.6	5.4	2.5	2.5

Remarks: ±, inhomogeneous in respect of the oxide analyzed. The grains analyzed are not the same as those on which the cell dimension and intergrowth study was done by the X-ray single-crystal method.

1. 76a/TK/63-1
2. 76a/TK/63-2
3. 89a/TK/63
4. 262/KV/64-1
5. 262/KV/64-2
6. 262/KV/64-3
7. 231a/KV/64

For characterization of rock samples, see Table 1.

of H_2O may have been higher. Instead of augite, hornblende was exsolved later on. If the augite was exsolved, it altered quickly into hornblende.

Tables 3, 4 and 5 show clearly that there are small, in some cases considerable, discrepancies in the composition estimates of the orthopyroxene derived by different methods. Because the X-ray, optical and electron microprobe determinations were made on different grains of orthopyroxene, the discrepancies may reflect a real inhomogeneity in composition, although the effect of interference by the exsolved phases on the composition is possible, too. The author trusts most in the X-ray single crystal data. In any event, the orthopyroxene shows a considerable composition range from bronzite through hypersthene to ferrohypersthene.

Augite

The mode of occurrence of the augite is similar to that of the hypersthene. Fig. 8 illustrates a typical augite. The mineral is met with in all the samples studied.

Most of the augite grains show a distinct »ribbon structure», the thin (1—2 μm) adjacent ribbons revealing a difference in relief under the microcsope. The ribbons are parallel to the (010) plane of the augite, *i.e.*, parallel to the optical axial plane. The ribbons seen in Fig. 9 represent possibly an intergrowth of augite and hornblende. This figure also illustrates a well-developed {001}-multiple twinning.

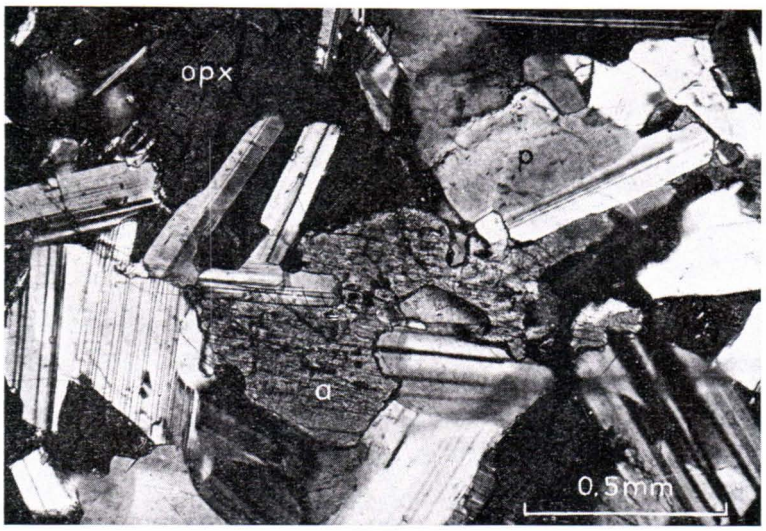

FIG. 8. Typical occurrence of augite (a) in gabbronorite. opx, lamellar orthopyroxene; p, plagioclase. The illustrated augite grain has $2V\gamma = 42°$ at margins and 36° in the core. Sample No. 89a/TK/63. Crossed nicols.

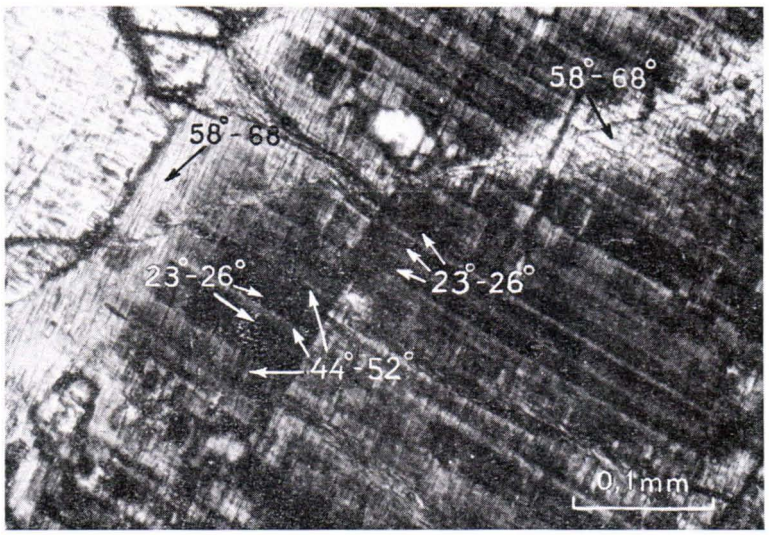

FIG. 9. Augite showing {001}-multiple twinning (lamellae from upper left corner to lower right corner) and perpendicular to the (001)-plane »ribbons», as discussed in the text. Some of the measured $2V\gamma$-values indicated in the photograph. Leuconorite, sample No. 262/KV/64. Crossed nicols.

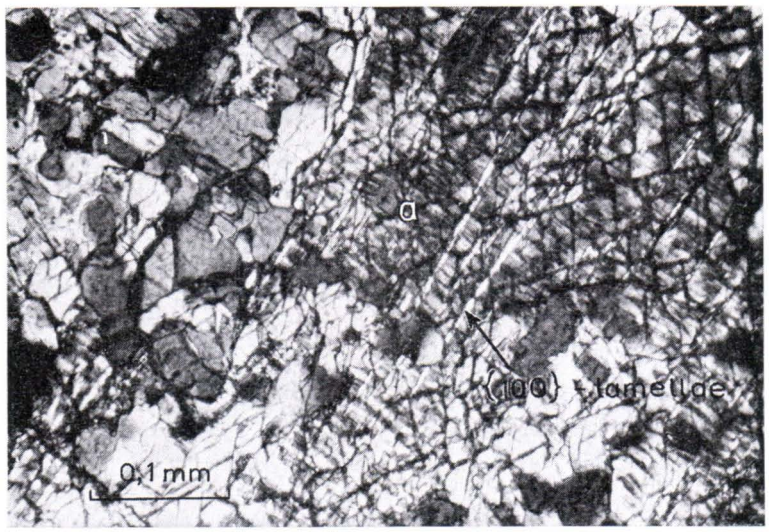

FIG. 10. {100}-hypersthene lamellae in augite (a). The ribbons, which are discussed in the text, can also be seen perpendicular to the {100}-lamellae. In the illustrated augite grain, the $2V\gamma = 54°$. Gabbronorite, sample No. 78b/TK/63. Crossed nicols.

Occasionally the augite is observed to contain well-developed hypersthene lamellae parallel to (100), as illustrated in Fig. 10. In the same grain, the »ribbon structure» is to be seen.

In some samples, the augite is complicately intergrown with hornblende. Figs. 11 and 12 illustrate an augite crystal rimmed by hornblende. Hornblende is also found as coherent splotches inside the augite crystal and as thin ribbons in the augite host. A similar intergrowth is illustrated in Figs. 13 and 14. In the author's opinion, the hornblende rim is an overgrowth and the ribbons are uralitization products.

Many of the augite grains were studied by using the Universal Stage. The fine-scaled multiple twinning and ribbon structure — produced by either replacement or exsolution — caused the axial angles measured to deviate sharply from those of augite. This is shown in Fig. 9. The thin section is almost perpendicular to the acute bisectrix. Hence the twin planes of the {001}-multiple twinned augite lie obliquely against the plane of the thin section. Owing to the thinness of the lamellae, the optical properties of adjacent twin lamellae intermingle. This may be the reason why the dark twin lamellae in Fig. 9 show a $2V\gamma$ (23°—26°) that is considerable smaller than that of the adjacent light lamellae ($2V\gamma = 44°$—52°). The untwinned margin and the portion around the crack in the upper right corner of the figure show $2V\gamma = 58°$—68°. These parts presumably represent recrystallized augite. Table 6 gives the $2V\gamma$ and $c \wedge \gamma$ of the augites studied. The determinations were made from different grains. When a range of $2V\gamma$ is observed in a single augite crystal,

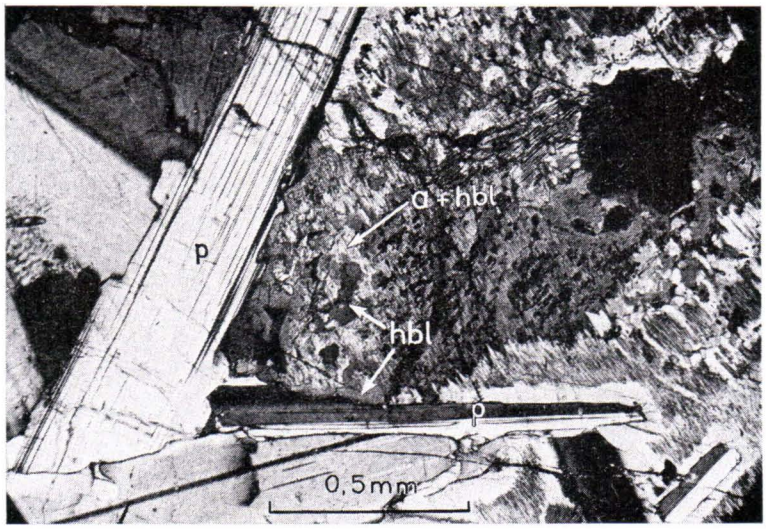

FIG. 11. Augite (a) intergrown with hornblende (hbl); p, plagioclase. For details, see text and Fig. 12. Gabbronorite, sample No. 231a/TK/65. Crossed nicols.

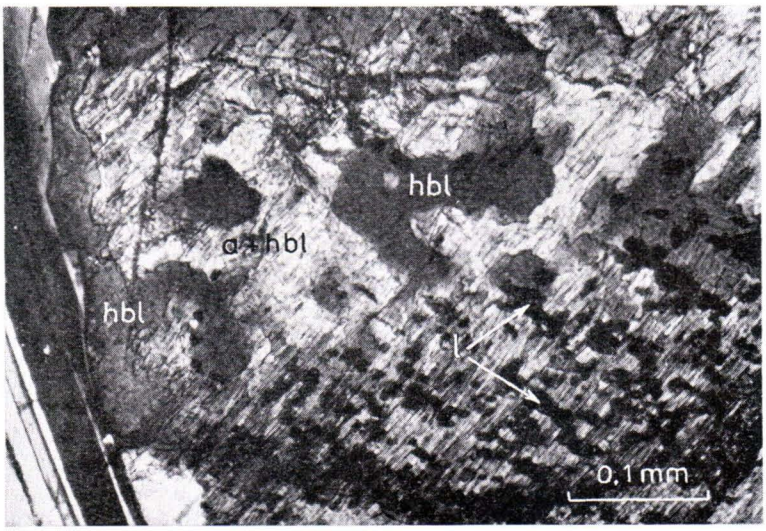

FIG. 12. Partial enlargement of Fig. 11, illustrating the augite (a) — hornblende (hbl) intergrowth. Symbol l indicates the ilmenite(?) exsolutions, partly altered into leucoxene. For details, see text. Crossed nicols.

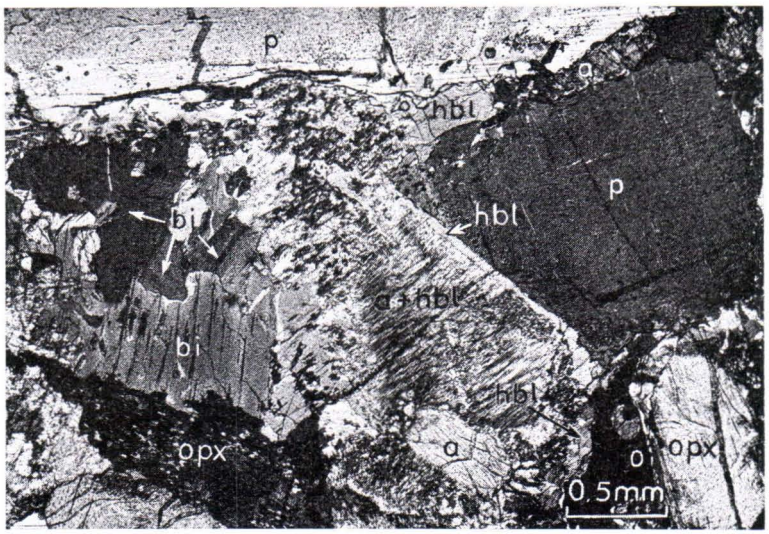

FIG. 13. Augite (a) intergrown with hornblende (a+hbl) and rimmed by hornblende (hbl). opx, orthopyroxene; bi, biotite; p, plagioclase; o, opaques. Gabbronorite, sample No. 76a/TK/63. Crossed nicols.

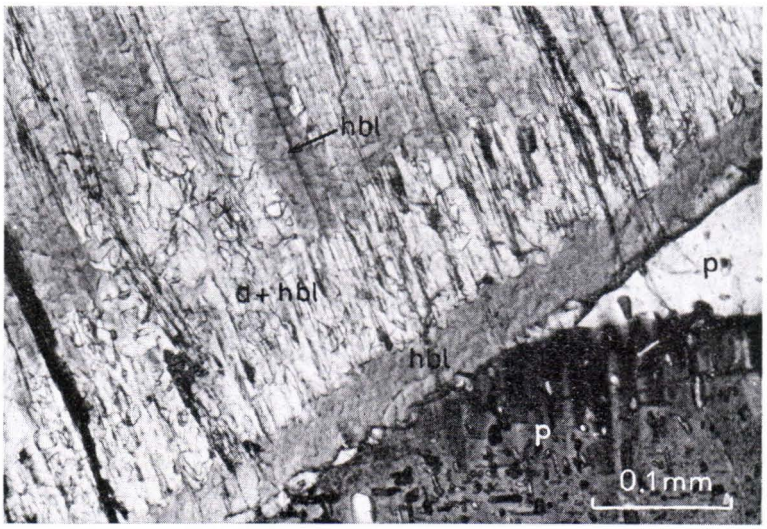

FIG. 14. A detail of Fig. 13. hbl, hornblende; a, augite; p, plagioclase. Crossed nicols.

TABLE 6.

Electron microprobe analyses, optical axial angles, extinction angles and cell dimensions of augites intergrown with hornblende, all from the norites of the Pieksämäki map sheet area.

	1	2	3	4	5	6	7
SiO_2	47.4	—	50.7	50.7	49.1	48.6	49.5
TiO_2	.3	—	.2	.3	.1	1.0	1.4
Al_2O_3	3.1	—	3.1	1.6	6.3	4.9	4.6
FeO	13.5	—	8.7	8.0	11.5	8.5	14.1
MnO	.2	—	.6	.2	.4	.2	.2
MgO	17.4	—	16.7	16.4	16.6	15.8	14.5
CaO	15.7	—	16.8	21.4	16.4	17.8	13.0
Na_2O	—	—	.9	—	.9	—	1.7
K_2O	—	—	.0	.3	—	—	.0
	97.6		97.7	98.9	101.3	96.8	99.0
Fe	20.9	—	14.5	12.4	18.5	14.3	24.9
Mg	48.0	—	49.6	45.2	47.7	47.4	45.7
Ca	31.1	—	35.9	42.4	33.8	38.3	29.4
$2V\gamma$	44°—56°, 44°—51°, 44°—63°, 44°—56°, 49°	54°	28°—32°, 36°—42°, 45°—54°, 36°, 56°	23°—68°, 54°—60°, 52°, 61°, 64°			59°
$c \wedge \gamma$	41°, 39°	40°	40°, 39°	40°, 41°			40°

	Augite	Hornblende
a_0	9.733 Å	9.846 Å
b_0	8.956	18.13
c_0	5.242	5.293
β	105°27′	104°59′

Chemically analyzed samples:

1. 76a/TK/63.
3. 89a/TK/63.
4. The homogeneous margin of finely twinned augite. 262/KV/64-1.
5. Augite with »ribbon structure» (augite + hornblende). 262/KV/64-2.
6. 262/KV/64-3.
7. Augite-amphibole intergrowth. 231a/KV/64.

Optically investigated samples:

1. Intergrown with hornblende (ribbon structure). See Fig. 14. 76a/TK/63.
2. Intergrown with hornblende (ribbon structure). 78b/TK/63.
3. 98a/TK/63. See also Fig. 8.
4—6. 262/KV/64. Some of the grains thinly twinned. See also Fig. 9.
7. 231a/KV/65. Complicated intergrowth with hornblende. See Fig. 12.

Cell-size determination:

7. 231a/TK/65. Augite-hornblende intergrowth.

For characterization of rock samples, see Table 1.

the result is $2V_{min}$ and $2V_{max}$. Most of the values obtained are characteristic of common augites. The very low values recorded (Nos. 262/KV/64 and 89a/TK/63) are presumably due to interference between the exsolved and twinned phases.

An augite crystal from sample 231a/KV/65 was studied by the single-crystal X-ray method by taking *a*- and *b*-axis zero-level precession photographs. Under the binocular microscope, the crystal splinter seemed to be homogeneous. The precession photograph showed the mineral to be a homoaxial intergrowth of clinopyroxene and amphibole, the reflections of both phases being equally strong. The intergrowth is probably similar to that illustrated in Fig. 12, which represents another augite of the same sample. It therefore seems that the »ribbon structure» of this augite is due to an augite-hornblende intergrowth. The cell dimensions of the intergrown clinopyroxene and hornblende are given in Table 6, Anal. 7.

Augites were also studied by the electron microprobe technique (Table 6). Excepting Anal. 4, which was made of the homogeneous margin of finely twinned augite, it is unlikely that any of the other analyses would represent the composition of augite alone. Anal. 5 is of an augite with a distinct »ribbon structure». Its very high Al_2O_3 content suggests a mixture of augite and hornblende. Anal. 6 is likewise of an augite-hornblende intergrowth.

The ribbons of the augite (Anal. 5) were scanned obliquely with an electron beam. The Si, Fe, Mg and Ca were recorded. The Mg content seemed to be constant while the simultaneous increase in Si and Ca contents was accompanied by a decrease in Fe, and vice versa.

The ribbons, the bulk composition of which is given in Anal. 6, were also scanned obliquely with an electron beam. The elements analyzed were Al, Fe, Mg and Ca. Also in this case, the Mg content was almost constant, but a simultaneous increase in Al and Fe was accompanied by a decrease in Ca, and vice versa. These fluctuations support the interpretation that an augite-hornblende intergrowth is really involved.

In places the augite contains small, darkish brown plate-like inclusions, as illustrated in Fig. 12. The inclusions are mainly translucent although opaque patches occur in spots. Inclusions in an augite-hornblende intergrowth from sample 231a/KV/65 were studied with the electron microprobe. The results showed a wide range in composition from one inclusion to another. This variation is caused by the thinness of the inclusion plates: they are considerably thinner than the thin section and the augite-hornblende intergrowth therefore has a strong influence on the analytical results. The chemical composition points to a mineral poorer in SiO_2, Al_2O_3, and richer in TiO_2 and CaO than the augite-hornblende host. It is likely that originally ilmenite was exsolved from augite, which was later replaced by leucoxene. Owing to the thinness of these exsolution lamellae, their optical properties are not characteristic of the typical leucoxene.

Amphiboles

The mode of occurrence of amphibole varies. It has been found to occur, for example:

— intergrown with augite as »ribbons». The cell dimension data for such an amphibole are given in Table 6, No. 7. The cell dimensions point to normal hornblende;

— as patches in augite (Fig. 12) and as marginal rims around augite. In both cases, the mineral is a homogeneous light green hornblende. The chemical composition of a hornblende rim is given in Table 7, Anal. 1. The Fe/Mg ratio in this rim is the same as in the augite (Table 6, Anal. 7);

— intergrown with orthopyroxene. A submicroscopical intergrowth is evidently in question. Possibly the augite exsolved from orthopyroxene was partly or completely replaced by amphibole. The cell dimensions (Table 4) suggest that the amphibole is hornblende;

— as a rim around orthopyroxene grains;

— as plagioclase-hornblende myrmekite (Fig. 15);

— as small grains of green hornblende, often seen to be ragged in form, either independent or as aggregates, where the grain size may be as small as 0.1 mm. The cell dimensions of one such grain are given in Table 8. These clearly correspond to those of the hornblende intergrown with orthopyroxene (Table 4, No. 7) from the same rock sample. The chemical composition of intercumulus hornblende from another rock sample is shown in Table 7, Anal. 2. The Fe/Mg ratio is considerably higher than that for the poikilitic augite of the same specimen (Table 6, Anal. No. 1),

TABLE 7.

Electron microprobe analyses of hornblendes and biotite from norites of the Pieksämäki map sheet area.

	1	2	3
SiO_2	48.3	41.8	38.9
TiO_2	1.1	3.6	5.2
Al_2O_3	6.4	8.9	15.8
FeO	13.9	16.4	16.3
MnO	.2	.2	.0
MgO	14.1	10.3	12.1
CaO	11.7	11.7	.1
Na_2O	.9	2.1	.3
K_2O	.5	1.5	8.6
	97.1	96.5	97.3
100 Fe/Fe+Mg+Mn	35.4	46.9	43.1

1. Hornblende; marginal rim around augite. 231a/KV/65.
2. Intercumulus hornblende. 76a/TK/63.
3. Intercumulus biotite. 76a/TK/63.

For characterization of rock samples, see Table 1.

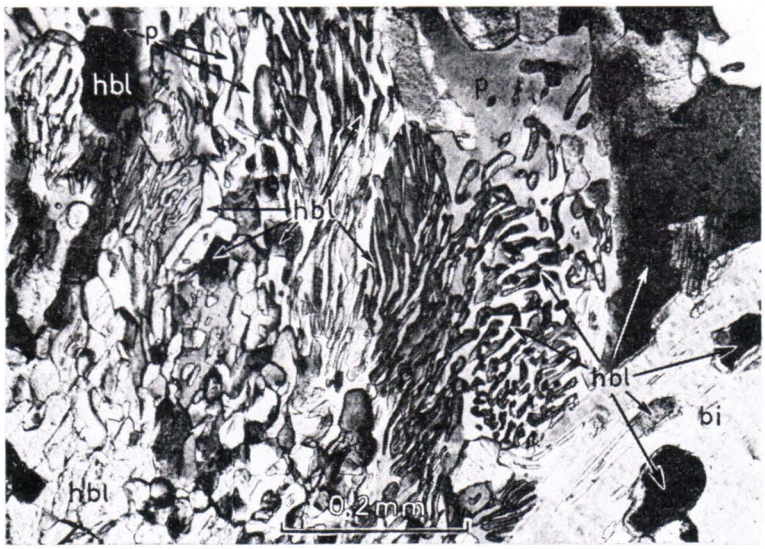

FIG. 15. Hornblende-plagioclase myrmekite. p, plagioclase; hbl, hornblende; bi, biotite. Gabbronorite, sample No. 231a/KV/65. Crossed nicols.

TABLE 8.

Cell size of hornblende, 10/PW/65.

$a_o = 9.866$ Å
$b_o = 18.14$
$c_o = 5.320$
$\beta = 105°02'$

For characterization of the rock sample, see Table 1.

suggesting that the intercumulus hornblende crystals crystallized at much lower temperatures than the augite;

— as small independent colourless amphibole (cummingtonite) grains, or as colourless amphibole intergrown with hornblende.

Amphibole may occur in all these ways even in a single sample. This shows that various submagmatic (deuteric), possibly also metamorphic, reactions took place to produce the amphibole, which is mostly normal hornblende. Of the reactions, the uralitization of augite seems to have been a two-fold process: the ribbon-structured intergrowth of augite and hornblende was produced first, then the homogeneous patches and the marginal rims of the hornblende in augite.

Most of the hornblende is light green (Z) to almost colourless (X) in thin section. Only the amphiboles in rock samples Nos. 10 and 13/PW, which are richer in iron, show more intense colours (Z = dark green, Y = brownish green and X = light

green, almost colourless). $2V\alpha$ varies greatly (72°—92°) and $c \wedge \gamma = 16° \pm 1$. An exception is the light green hornblende from the strongly epidotized sample 78b/TK/63, in which $c \wedge \gamma = 12°$. Lamellar {100}-twinning is common.

Biotite

Not only hornblende but also biotite occurs in various ways in the norites studied. Most commonly the biotite occurs as intercumulus flakes and aggregates. Some of the intercumulus flakes are quite small, and some are large poikilitic flakes that in many cases accompany augite, possibly as a partial replacement product. In some instances, biotite is found only as parallel owergrowth flakes on hypersthene (Figs. 4 and 5). Some of the samples are thoroughly devoid of biotite.

The intercumulus biotite is often accompanied by ore grains. Especially when intercumulus biotite forms aggregates, there are opaque grains present in abundance.

The colour of biotite in all cases is reddish brown, indicating a low Fe_2O_3/Fe_2O_3+ FeO ratio, possibly combined with a high TiO_2 content (*cf.*, Hayama 1959, Rimšaite 1967).

An electron microprobe analysis (Table 7, Anal. 3) was made of a small intercumulus biotite fiake from sample No. 76a/TK/63. The analyzed fiake is shown in Figure 3 (arrow indicated by *bi*). In the same figure, also the chemically analyzed grains of hornblende (Table 7, Anal. No. 2), augite (Table 6, Anal. No. 1), and orthopyroxenes (Table 5, Anal. Nos. 1 and 2) are indicated by arrows. The biotite analysis shows a very high TiO_2 content, 5.2 %. This indicates possibly a high equilibration temperature for this mineral.

Table 7 shows the iron-magnesium ratio in hornblende and biotite to be about the same. The distribution coefficient of iron between hornblende and biotite is thought to be quite constant (see, *e.g.*, Saxena 1968, Hietanen 1971). It cannot be said therefore whether the biotite and hornblende of sample 76a/TK/63 crystallized concurrently. Nor can it be definitely judged whether they are the result of magmatic or submagmatic crystallization. The author thinks it more likely that both originated at submagmatic temperatures.

COEXISTING PYROXENES

From the orthopyroxene analyses in Table 5 and clinopyroxene analyses in Table 6, the atomic ratios Fe : Mg : Ca have been calculated and plotted on the pyroxene quadrilateral (Fig. 16). Owing to the presence of exsolved and/or replaced phases, the analyzed minerals are not pure. If the analytical data given represented the compositions of the minerals in equilibrium before the exsolution, there should be no intersecting tie lines in the diagram when the composition points of coexisting

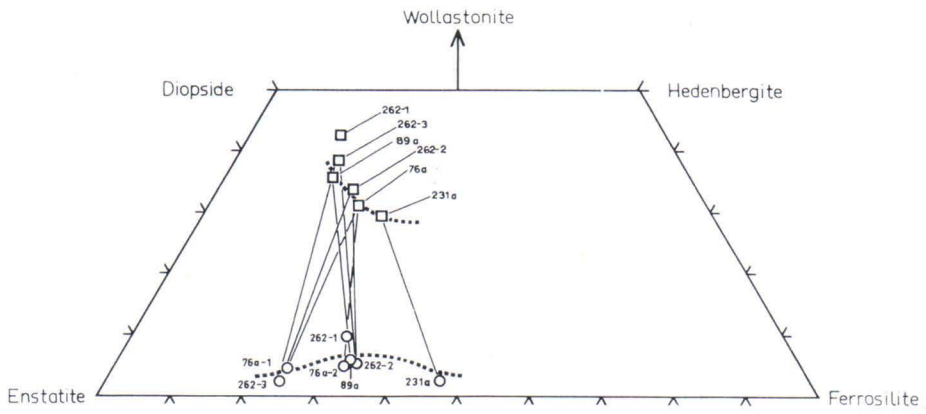

FIG. 16. The coexisting orthopyroxenes and clinopyroxenes plotted in the pyroxene quadrilateral.

orthopyroxene and clinopyroxene are connected. The intersecting tie lines in the diagram point to a disequilibrium in the Fe/Mg distribution between the pyroxene phases in question and to migration of elements on a large scale either during the deuteric stages, after the main magmatic crystallization, or during the regional metamorphism, when partial recrystallization of the rocks took place. The homogeneous clinopyroxene (No. 262/KV/64-1) along the margin and adjacent to the crack of the thinly twinned augite, seems to have been equilibrated at much lower temperatures than the other pyroxenes.

If the schematically outlined solvus in Fig. 16 is real, then the crystallization temperature is quite high, comparable to that of the Skaergaard intrusion (see, *e.g.*, Wager and Brown, 1967, p. 39, Fig. 19). This comparison pays attention only to the width of the solvi.

ACKNOWLEDGMENTS

The author received valuable aid from Mr. Pentti Ojanperä, M.Sc. (wet chemical analysis), Miss Tuula Paasivirta, M.Sc. (electron microprobe analyses), Mr. Matti Vaasjoki, M.Sc. (X-ray study of the hornblende-augite intergrowth), Mr. Erkki Halme (photographs), Mrs. Anni Vuori (who drew the sketch map and lettered the mineral symbols on the photographs), Miss Liisa Siren (who drew diagram in Fig. 16).

Professor Ahti Simonen and Dr. Kai Hytönen read the manuscript critically and made suggestions that led to some improvements. Dr. Marjatta Okko's editorial reading of the manuscript proved of great value, resulting in improvements and revisions in the text. Mr. Paul Sjöblom, M.A., corrected the English of the manuscript.

Received December 30, 1974.

REFERENCES

DEER, W. A., HOWIE, R. A. and ZUSSMAN, J. (1963) Rock-forming Minerals, Vol. 2, Chain Silicates. 379 p., Longmans.

GAÁL, GABOR (1972) Tectonic control of some Ni-Cu deposits in Finland. 24th IGC, Section 4, 215—224.

—»— and RAUHAMÄKI, E. (1971) Petrological and structural analysis of the Haukivesi area between Varkaus and Savonlinna, Finland. Bull. Geol. Soc. Finland 43, 265—337.

HÄKLI, T. A. (1968) An attempt to apply the Makaopuhi nickel fractionation data to the temperature determination of a basic intrusive. Geochim. Cosmochim. Acta 32, 449—460.

—»— (1970) Factor analysis of the sulphide phase in mafic-ultramafic rocks in Finland. Bull. Geol. Soc. Finland 42, 109—118.

—»— (1971) Silicate nickel and its application to the exploration of nickel ores. Bull. Geol. Soc. Finland 43, 247—263.

HAYAMA, YOSHIKAZU (1959) Some considerations on the color of biotite and its relation to metamorphism. J. Geol. Soc. Japan 65 (760), 21—30.

HIETANEN, ANNA (1971) Distribution of elements in biotite-hornblende pairs and in an orthopyroxene-clinopyroxene pair from zoned plutons, Northern Sierra Nevada, California. Contr. Mineral. and Petrol. 30, 161—176.

HYVÄRINEN, LAURI (1969) On the geology of the copper ore field in the Virtasalmi area, eastern Finland. Bull. Comm. Géol. Finlande 240, 82 p.

KAHMA, AARNO (1973) The main metallogenic features of Finland. Geol. Surv. Finland Bull. 265, 28 p.

RIMŠAITE, J. H. Y. (1967) Studies of rock-forming micas. Geol. Surv. Canada Bull. 149, 82 p.

SALTIKOFF, BORIS (1971) Virtasalmen alueen emäksisten kivien nikkelipitoisuudesta. Manuscript in the Archives of the Geological Survey of Finland.

SAVOLAHTI, ANTTI (1966) Some features of the Salmenkylä gabbro in Kangasniemi commune, Finland. Bull. Comm. Géol. Finlande 222, 109—115.

SAXENA, S. K. (1968) Crystal-chemical aspects of distribution of elements among coexisting rock-forming silicates. N. Jb. Mineral., Abh. 108 (3), 292—323.

STRECKEISEN, ALBERT L. (1973) Plutonic rocks, classification and nomenclature recommended by the IUGS subcommission on the systematics of igneous rocks. Geotimes 18 (10), 26—30.

VORMA, ATSO (1971) Map of Pre-Quaternary rocks, sheet 3232, Pieksämäki. Geological Map of Finland, 1 : 100 000.

WAGER, L. R. and BROWN, G. M. (1967) Layered igneous rocks. Oliver and Boyd, London. 588 p.

WAHL, WALTER (1963) The hypersthene granites and unakites of Central Finland. Bull. Comm. Géol. Finlande 212, 83—100.